Nanogranular SnO₂ Layers for Gas Sensing Applications by In Situ Deposition of Nanoparticles Produced by the Karlsruhe Microwave Plasma Process

Benedikt Schumacher,* Rolf Ochs, Harald Tröße, Sabine Schlabach, Michael Bruns, Dorothée V. Szabó, Jürgen Haußelt

To improve the performance of the central element of the Karlsruhe Micronose — a gas-sensor microarray — the gas sensitive layer is modified toward a highly porous nanogranular layer. To synthesize those layers, the Karlsruhe Microwave Plasma Process which is in its native form a precursor-based process to produce nanoparticles with diameters below 10 nm, was modified for in situ tin-dioxide layer deposition. The produced layers have due to their structure a very large active surface area. The process parameters were optimized to generate thin layers with high surface homogeneity. This was mostly established by significantly reducing the precursor feed and therefore reducing the primary particle size to below 2 nm. The layers were analyzed for their mechanical stability, structural, and chemical properties. It is shown that the precursor residue can be completely removed by applying a default annealing step. The structure of the layers reminds of little clubs starting on top of the substrate growing wider toward the surface. Prototype sensors were fabricated and tested for their gas sensory properties in comparison to a standard gas-sensor microarray with a sputtered tin-dioxide layer. The gas-sensor microarrays with nanogranular layer show an increased signal response of up to one order of magnitude to isopropanol. The time of response is equal in both sensor systems while the time of recovery is nearly doubled for the sensors with nanogranular layer due to increased surface area and gas absorption.

Introduction

The Karlsruhe Micronose (KAMINA) was developed at the Forschungszentrum Karlsruhe (Karlsruhe Research Centre) and is now on its way to industrial production and application.[1,2] The central element of the KAMINA is a gas-sensor microarray (GSMA) with up to 39 electrodes (Figure 1) — differentiated by a temperature gradient and a silicon-dioxide gradient membrane — on top of a sputtered metal-oxide layer with a thickness of about 150 nm. The electrical conductivity of the metal-oxide layer is highly sensitive to the composition of the ambient gas atmosphere. The basic structures of the microarray cover a chip area of 4×8 mm^2 on the 9×10 mm^2 substrate and are manufactured by radio frequency (RF) magnetron sputtering, applying a shadow mask technique. The parallel platinum strip electrodes are sputtered on top of the metal-oxide, thus separating the latter into the initially equal sensor elements.

One way to further improve the gas sensing abilities of the GSMA is to increase the actively sensing metal-oxide

B. Schumacher, R. Ochs, H. Tröße, S. Schlabach, M. Bruns, D. V. Szabó, J. Haußelt
Forschungszentrum Karlsruhe, Institut für Materialforschung III, Hermann von Helmholtz Platz 1, 76344 Eggenstein Leopoldshafen, Karlsruhe, Germany
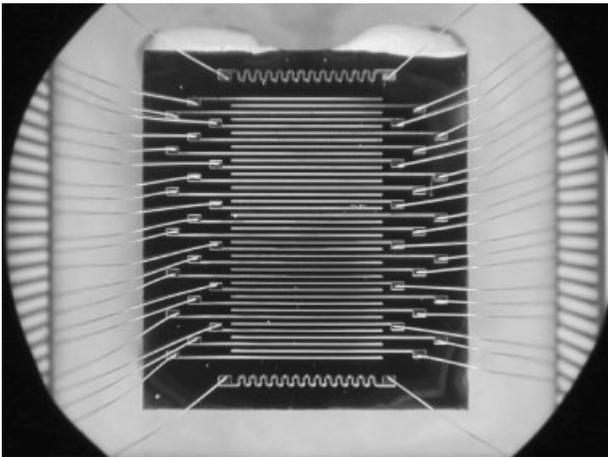E mail: benedikt.schumacher@imf.fzk.de

Figure 1. Photograph of a GSMA bonded onto a pin grid array (PGA).

surface area by not increasing the used chip area. The signal strength of metal-oxide gas-sensors can be improved further by decreasing the crystallite size of the used metal-oxide as proposed by Schaumburg and Teubner in 1992[3] and reported by Kennedy et al. in 2003.[4] One method is to apply nanoparticles via spin-coating,[5] drop-coating,[6,7] or screen-printing.[7,8] Deposition processes using colloidal solutions of nanoparticles poses the problem of particle growth, as one has to eliminate the binding phase by a temperature treatment.

The Karlsruhe Microwave Plasma Process (KMPP) is a versatile plasma process capable of producing nanoparticles with primary particle sizes below 10 nm and a very narrow particle size distribution.[9] Water-free precursors (chlorides, carbonyls or alcoxides) with an evaporation temperature below 300 °C are used as starting materials. Depending on the choice of the precursor and the reaction-gas, oxides, or nitrides can be formed. Furthermore, the process can be configured to produce ceramic/ceramic core–shell particles. Ceramic particles coated with a different ceramic layer (e.g., tin-dioxide core with a silicon-dioxide shell) are expected to show significantly reduced particle growth due to the barrier. This is a very promising approach to prevent the functional particles from growing.[10] As the operating temperature of the GSMA is in the range of 300 °C, this is important to prevent aging of the sensor. Therefore, particle growth has to be eliminated up to these temperatures.

As with this process nanoparticles are deposited in situ from the gas-phase onto substrates, liquid binding phases are avoided. This may reduce influence from the binding phase on the sensor performance and is an advantage. It is the aim of this paper to prove the concept of nanogranular gas sensitive layers based on SnO_2 and SnO_2/SiO_2 nanoparticles directly deposited from the gas phase onto the GSMA of the KAMINA.

This paper focuses on the comprehensive characterization of nanoparticles and nanogranular thin films using transmission electron microscopy (TEM), X-ray diffraction (XRD), scanning electron microscopy (SEM), and X-ray photoelectron spectroscopy (XPS). The sensor properties of the manufactured prototype GSMA are analyzed in pulsed gas exposure experiments in comparison to sputtered SnO_2 layers.

Experimental Part

A new substrate holder was developed to expand the existing KMPP equipment. It allows introducing two substrates (9×10 mm^2) simultaneously into the particle stream and controlling the time of exposure. For quality control by means of XPS one version of the substrate holder allows borderless coating of silicon test substrates. For KAMINA application a substrate holder with a shadow mask was constructed to allow the deposition of the nanostructured layers by preventing the bond pads and temperature sensors from being coated (cf. Figure 1). The substrate holders are made out of brass and surrounding customized glassware for vacuum closeness. They allow to coat up to eight substrates during one process run.

Tin dioxide was chosen as the metal-oxide since it is the standard material used in KAMINA. As precursor material for the SnO_2 tin-IV-chloride [Fluka order-#: 96560, purum p.a.; Assay > 98.0% (AT)] was selected for its chemical and physical properties. The resulting layers are to be free of any unwanted precursor residue. With chlorine being the only binding partner of tin, $SnCl_4$ proved to be a good choice for the synthesis of gas-sensory active SnO_2 layers. As a liquid $SnCl_4$ is easy to dose at room temperature using a syringe pump (KD Scientific) and the evaporation temperature of about 114 °C is easy to achieve. The only drawback is that $SnCl_4$ has to be handled in dry inert-gas atmosphere to prevent reactions with water vapor in the air. The used process gas was an argon/oxygen mixture (oxygen 4.8, argon 5.0, Messer Group GmbH, 20 vol.-% oxygen) as the reaction gas and argon (argon 6.0, Messer Group GmbH) as the carrier gas for the evaporated precursor.

As the microwave plasma source, a 2 kW 2.45 GHz magnetron (Muegge Electronic GmbH, Reichelsheim, Germany) with isolator and tri-stub tuner were used. A reaction tube, made of quartz glass, passes the microwave cavity that is operated in rotating TE_{11}-mode. At the intersection, the plasma is ignited. The $SnCl_4$ is evaporated outside the microwave cavity and reacts with the reaction gas within the microwave plasma. The residence time within the plasma zone is only a few milliseconds and the temperature of the plasma usually below 500 °C. Therefore, the produced nanoparticles are very small. The rig is described in detail in ref.[9]

The layers were produced using a microwave power of 460 W, a total gas flow of 10.4 l min^{-1}, a system pressure of about 1 200 Pa, and a gas temperature behind the plasma zone of 350–450 °C. The thermal evaporator for the $SnCl_4$ was kept at an operating temperature of 140 °C. With these process parameters, thin and homogenous layers of nanogranular SnO_2 could be reproducibly manufactured on top of silicon substrates.

The layers were analyzed using SEM (ISI SR-50A at 15 kV and LEO 1530 at 10 kV) and XPS (VG Clam 100, MgKα at 200 W, 20 eV narrow scan pass energy). For particle characterization by TEM (FEI Tecnai F20ST at 200 kV) and helium pycnometry (Micromeritics Accu-Pyc 1330), powder was collected in parallel to the layer deposition.

The optimized layers were deposited on top of pre-structured GSMA substrates by protecting the bond pads and temperature sensors from being coated using a shadow mask. On the reference sensor with a sputtered SnO_2 layer, the platinum electrodes are on top of the metal-oxide. The nanogranular metal-oxide is deposited on top of the platinum electrodes, since the highly porous layers were not expected to be rigid enough to support the platinum. Therefore, the electrodes were applied to the silicon substrate before the metal-oxide layer deposition. This setup has the drawback that the test gases have to diffuse through the metal-oxide before being detected. The penetration is mostly based on diffusion effects. To reduce the time of response to a minimum, thin layers had to be achieved. The advantage of this setup is that prototype production time could be cut by not having to worry about the mechanical strength of the newly developed layers.

Prototype GSMA with nanoporous SnO_2 layer were pulsed gas exposure tested after the bonding process using carbon monoxide (CO 1.8 1971 ppm ± 2% in synthetic air, Messer Group GmbH) and isopropanol [C_3H_8O 501 ppm ± 2% in nitrogen (N_2) 5.0, Air Liquide Deutschland GmbH, Düsseldorf, Germany] atmosphere with defined gas concentrations (1, 5, 10, 50, and 100 ppm each after a proceeding 0 ppm measurement) in comparison to a standard GSMA with a sputtered SnO_2 metal-oxide layer. The relative humidity of the gas atmosphere was 50% rel. for all the gas-sensoric tests. Synthetic air (21.0 vol.-% oxygen 79.0 vol.-% nitrogen, Basi Schöberl GmbH, Rastatt, Germany; 20.5 vol.-% oxygen 79.5 vol.-% nitrogen, Air Liquide Deutschland GmbH) was used for diluting the test gases and for cleaning of the gas mixing rig.

First experiments were conducted to prove the expectation that coated nanoparticles show reduced crystallite growth behavior. As test materials non-coated SnO_2 particles and SiO_2-coated SnO_2 particles with a coating thickness of approx. 0.5 nm were produced under comparable conditions. These two materials were then annealed at 300 °C for a period of 21 days, respectively. Sampling was performed after 0, 3, 7, 14, and 21 days. The samples were analyzed with respect to crystal growth using XRD (Philips X'Pert, CuKα radiation). The crystallite size was then determined using the Scherrer formula.[11]

Results and Discussion

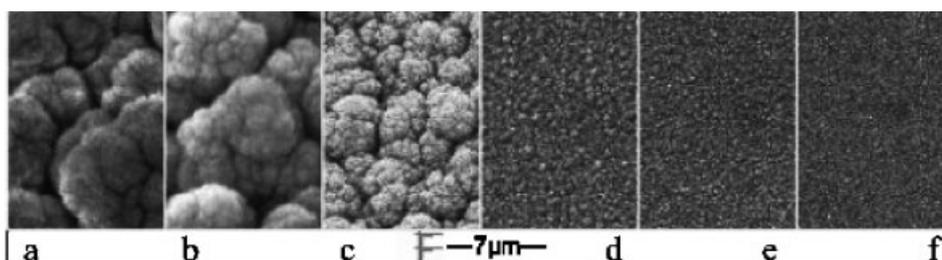The main parameter responsible for the thickness and uniformity of the layers

Figure 2. SEM images of the surface topography of nanogranular SnO_2 layers produced with different precursor concentrations [(a,b): 2.2×10^{-4} mol l⁻¹; (c): 1.1×10^{-4} mol l⁻¹; (d): 2.8×10^{-5} mol l⁻¹; (e): 1.4×10^{-5} mol l⁻¹; (f): 5.5×10^{-6} mol l⁻¹].

is the precursor concentration in the reaction gas. Best results could be achieved using precursor concentrations of 2.8×10^{-6} mol·l⁻¹ (corresponding to a $SnCl_4$ feeding rate of 0.1 ml·h⁻¹ and a reaction gas flow of 5.2 l·min⁻¹) which is the lowest concentration achievable with the currently used equipment. With decreasing precursor concentration in the reaction gas stream, a reduction in the sizes of cauliflower-like structures is observed. The layers exhibit high uniformity (Figure 2).

Reproducibility of layers was achieved by preheating the substrate holder in the particle free hot gas stream leaving the plasma zone. The temperature of the substrate holder before layer deposition was in the range of 400 °C. In the current setup it was not possible to actively regulate the substrate temperature. The surface topography strongly depends on the temperature of the substrate (Figure 3). On the cold substrate large aggregates are formed whereas a preheated substrate shows small and homogenous particle aggregates on the surface.

Layers as thin as 200 nm (determined by SEM) exhibiting a homogenous surface could be produced by depositing nanoparticles for 1 min at 2.8×10^{-6} mol·l⁻¹ onto a preheated substrate. To get an idea of the topography of the layers SEM was used to take pictures of freshly broken edges. The layers consist of little clubs and needle-like structures [Figure 4(b)]. They start on top of the substrate growing wider toward the surface of the layer.
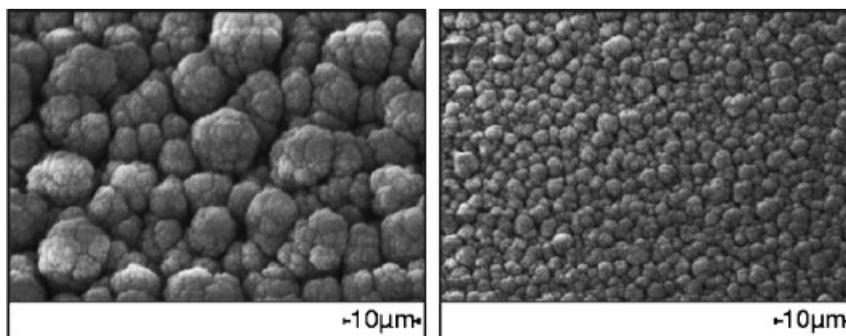

Figure 3. SEM images of the surface topography of a layer deposited onto a cold substrate (left) and a hot substrate (right) at equal precursor concentrations.
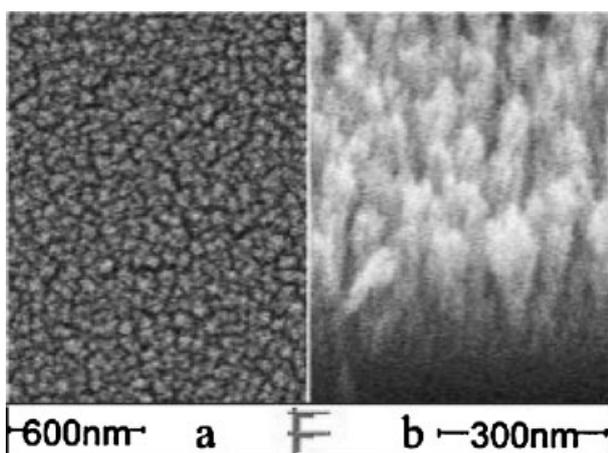
Figure 4. SEM images of an SnO₂ nanogranular layer (a) top view and (b) view at an angle of 45°.

The round ends of the clubs result into the impression of cauliflower-like structures in top view [Figure 4(a)].

TEM analysis revealed that the primary particle size of the powder particles is reduced from below 5 nm to below 2 nm by reducing the precursor concentration from 5.5×10^{-4} to 2.8×10^{-6} mol·l^{-1}. The larger powder particles, produced with high precursor concentrations, can be classified as Cassiterite by TEM diffraction patterns in reference to JCPDS 41-1445 (Figure 5, left). For the small powder particles, produced with low precursor concentrations, the diffraction rings are too wide to be clearly separated (Figure 5, right), but lattice fringes found in high resolution images can still be assigned to lattice planes of
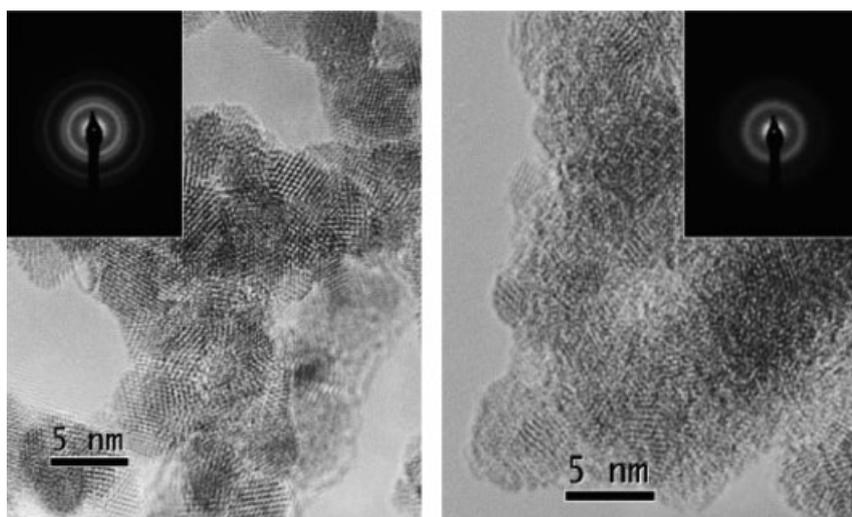
the Cassiterite. Dark field TEM images reveal that all the collected SnO₂ powders are crystalline. The particle size is significantly smaller as seen in the particle size of sensor layers made by gas phase condensation[4,12] or flame spray pyrolysis.[13]

Helium pycnometry measurements revealed a density of the separately collected powder of 6.8–7.0 g·cm^{-3} which is in the range of the theoretical value of 6.992 g·cm^{-3} for bulk SnO₂.

It was shown by XPS analysis, that the as-deposited layers show a significant content of chlorine — residue of the precursor. The chlorine can fully be removed by a succeeding tempering step of three days at 300 °C (the operating temperature of the GSMA) in air (Figure 6) for all the samples. This tempering step is a default production step in GSMA manufacturing. To reveal the chemical state of the chlorine, temper experiments in ultra high vacuum have been conducted at 300 °C, during which the chlorine content did not change. This suggests that the chlorine is still bound to the Sn and not only absorbed on the surface of the SnO₂. The chlorine needs to be substituted by oxygen in order to leave the layer. After the tempering process only signals of tin, oxygen, and adventitious carbon can be detected in the layers made of bare SnO₂ nanoparticles deposited onto Si test substrates. Since no silicon peaks were found in the spectrum, the layers cover the whole substrate and exhibit no holes or cracks.

Gas-analytical tests revealed that the generated SnO₂ layers are gas-sensory active. The expected enhancement of the signal could be proved for the case of isopropanol test gas atmosphere (Figure 7, left). In this case, the resulting signal was about one order of magnitude higher as the signal of the reference sensor. For the tests in carbon monoxide test gas atmosphere both sensors showed nearly equal signal responses to different carbon monoxide concentrations (Figure 7, right).

The time of response (t_{90}) was determined to be in the range of 0.4 min for both sensor systems. This was not to be expected since the surrounding gas atmosphere has to penetrate the metal-oxide layer by diffusion in the case of the nanogranular layer. The high porosity seen in SEM images can therefore be proved by the sensor response of the GSMA. Due to increased surface area, the recovery time of the nanogranular sensor is nearly doubled in comparison to the sensor with sputtered SnO₂ layer.

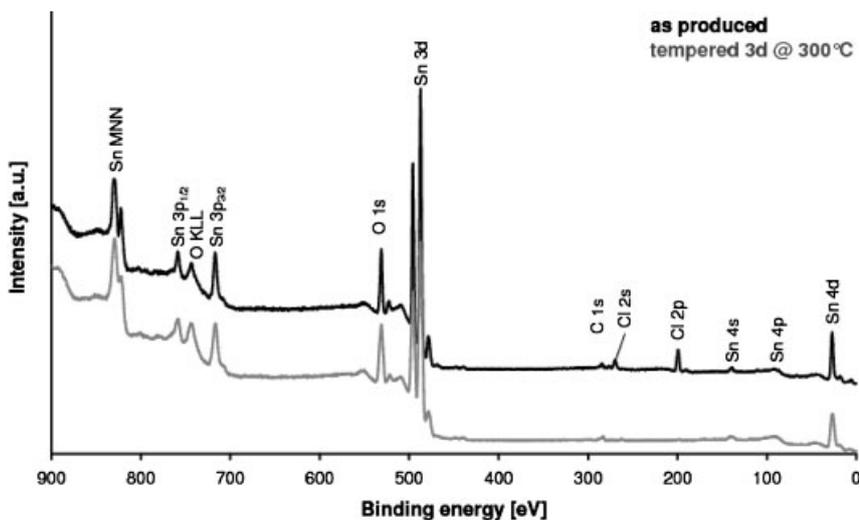The crystal growth experiments using non-compacted powders show

Figure 5. TEM images of SnO₂ powders produced with different precursor concentrations. Left: 5.5×10^{-4} mol l^{-1}. Right: 3×10^{-6} mol l^{-1}. Lattice fringes can be seen in both images. The insets (top left, respectively top right corner) show the diffraction image of the powder sample shown in the image. As a result from very small primary particles excessive line broadening is observed in the top right inset.

Figure 6. XPS spectra of nanogranular tin dioxide layer on silicon substrate. Black: as deposited. Gray: after tempering for three days at 300°.

ment, using SnO_2 nanoparticles coated with ca. 0.5 nm thin SiO_2 shell shows that core–shell SnO_2/SiO_2 powder particles exhibit reduced crystal growth compared to uncoated SnO_2. After 21 days, the primary crystallite size of the core is still below the size of the bare SnO_2 (Figure 8). Therefore, it is demonstrated that coating may reduce the crystal growth, but the thickness of the coating has still to be optimized with respect to particle growth as well as sensor performance. The sensor activity of SiO_2 coated SnO_2 is currently under investigation. Experiments on the crystal growth in nanogranular layers instead of compacted powder are on the way.
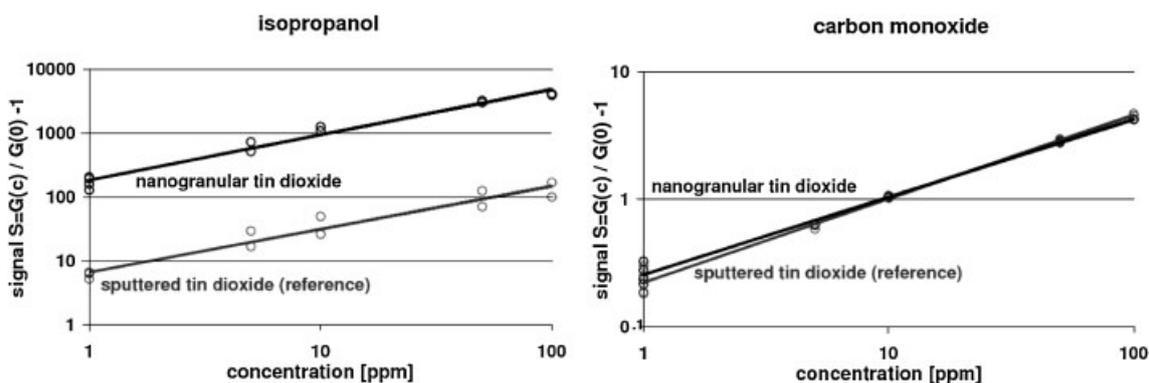
Figure 7. Signal response of sensor with nanogranular SnO_2 layer and of sensor with sputtered SnO_2 layer (reference) for different concentrations of isopropanol (left) and carbon monoxide (right) during gas pulse exposure tests.

that bare SnO_2 powder particles grow rapidly from below 2 nm to about 4 nm within one week. The expected sensor degradation due to crystal growth could not be observed during the short-term testing interval of 3 weeks. The sensors were kept at the operation temperature (275–325 °C gradient) at all times. A primary crystallite size of 4 nm — as seen in the crystal growth experiments — seems to be sufficiently small enough to detect changes in the surrounding gas atmosphere with highly increased signal responses in comparison to sputtered layers. The layers are mechanically stable and defy tab and tape tests but they are not yet scratch resistant.

For long-term stability of the gas analytical performance, crystal growth and agglomeration of the functional particles have to be avoided. A very promising approach therefore is to use core–shell nanoparticles. It is known that ceramic/ceramic core/shell nanoparticles show only little grain growth for the core phase during sintering as the coating acts as a diffusion barrier.[10] A first experi-
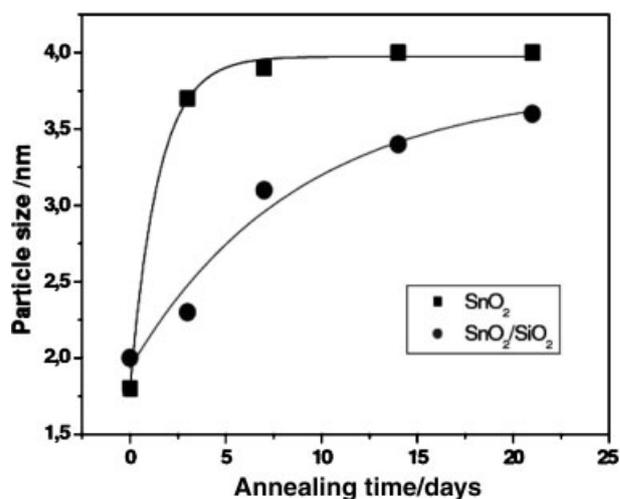

Figure 8. Particle growth of loosely compacted SiO_2 coated (dots) and non coated (squares) SnO_2 powder particles at 300 °C over a period of 21 days.

Conclusion

The KMPP proved to be a flexible tool for producing nanogranular highly porous layers. The experimentally gained process parameters allow fabricating reproducible hole- and crack-free layers with a thickness of about 200–500 nm. Residual chlorine from the precursor material can be totally eliminated by a succeeding tempering step. The mechanically stable layers are chemically and electronically active and exhibit enhanced functionality in comparison to their sputtered counterparts.

The novel technology could easily be integrated into the existing microsystem KAMINA and proved to be a possible route to improve the performance of established GSMA equipment. With respect to long-term stability, coated nanoparticles seem to be a promising choice to manufacture highly sensitive GSMA with significantly reduced aging effects.

[1] J. Goschnick, *Microelectron. Eng.* **2001**, *57–58*, 693.

[2] SYSCA AG; Im Köbler 2, D75438 Knittlingen; Germany (www.sysca-ag.de).

[3] H. Schaumburg, *"Werkstoffe und Bauelemente der Elektronik 3: Sensoren"*, B. G. Teubner, Stuttgart **1992**, p. 444 ff.

[4] M. K. Kennedy, F. E. Kruis, H. Fissan, B. R. Mehta, S. Stappert, G. Dumpich, *J. Appl. Phys.* **2003**, *93*, 551.

[5] J. Gong, Q. Chen, W. Sei, S. Seal, *Sens. Actuators* **2004**, *B102*, 117.

[6] T. Sahm, L. Mädler, A. Gurlo, N. Barsan, S. E. Pratsinis, U. Weimar, *Sens. Actuators B* **2004**, *98*, 148.

[7] T. Sahm, L. Mädler, A. Gurlo, N. Barsan, S. E. Pratsinis, U. Weimar, *Mater. Res. Soc. Proc.* **2005**, *828* A1.3.1.

[8] M. C. Carotta, A. Giberti, V. Guidini, C. Magalù, B. Vendemiati, G. Martinelli, *Mater. Res. Soc. Symp. Proc.* **2005**, *828*, A4.6.1.

[9] D. Vollath, V. Szabo, "Synthesis of Nanopowders by the Microwave Plasma Process — Basic Considerations and Perspectives for Up Scaling", in: *Innovative Processing of Films and Nanocrystalline Powders*, K.-L. Choy, Ed., Imperial College Press, London, UK 2002, p. 219 ff.

[10] D. Vollath, D. V. Szabó, J. Haußelt, *J. Eur. Ceram. Soc.* **1997**, *17*, 1317.

[11] P. Scherrer, *Nachrichten von der Gesellschaft der Wissenschaften zu Göttingen* **1918**, 98.

[12] J.-P. Ahn, J.-H. Kim, J.-K. Park, M.-Y. Huh, *Sens. Actuators* **2004**, *B99*, 18.

[13] L. Mädler, T. Sahm, A. Gurlo, J.-D. Grunwald, N. Barsan, U. Weimar, S. E. Pratsinis, *J. Nanoparticle Research* **2006**, *8*, 783. doi:10.1007/s11051–005–9029–6.